EXPERIMENTAL ANALYSIS OF PLUTONIUM PRODUCT AND RAFFINATE WASTE STREAMS FROM A PUREX PROCESS ON A LOW BURN-UP, FAST NEUTRON IRRADIATED DUO2 PELLET

A Thesis

by

JARROD RYAN ALLRED

Submitted to the Office of Graduate and Professional Studies of
Texas A&M University
in partial fulfillment of the requirements for the degree of

MASTER OF SCIENCE

Chair of Committee,	Sunil S. Chirayath
Co-Chair of Committee,	Charles M. Folden III
Committee Member,	David R. Boyle
Head of Department,	Yassin A. Hassan

August 2016

Major Subject: Nuclear Engineering

ABSTRACT

Experimental investigations of separating actinides (uranium and plutonium) from fission products (FP) were conducted using a modified Plutonium Uranium Recovery by Extraction (PUREX) process. The sample under investigation was a low-burn-up (< 5 GWd/tHM), depleted uranium dioxide (DUO_2) sample (~13 mg) irradiated in a fast neutron spectrum in the High Flux Isotope Reactor (HFIR) at Oak Ridge National Laboratory (ORNL). The objective of the study was to quantify the fission product decontamination factor for PUREX process steps while separating and purifying plutonium. Aliquots of the dissolved neutron-irradiated DUO_2 sample containing FPs and near weapons-grade plutonium (~ 89% ^{239}Pu), underwent three modified PUREX decontamination cycles with products (organic and aqueous solutions) from each process step being analyzed via high-resolution gamma spectroscopy. The purification cycle consisted of tri-n-butyl-phosphate (TBP) and kerosene contacted with the feed solution aliquot to extract actinides (plutonium and uranium primarily) from feed to organic phase and further actinide (plutonium only) back-extraction using ferrous sulfamate. Fission product elements, cesium (by measuring ^{137}Cs) and cerium (by measuring ^{144}Ce) were determined to be the most readily removed elements from the product stream when analyzing a whole plutonium purification cycle. The nuclides that posed the greatest difficulty in removal included zirconium (by measuring ^{95}Zr) and ruthenium (by measuring ^{106}Ru) through the 1^{st} cycle of the purification.

The results of this study could be useful in nuclear forensics analysis in the event of a plutonium smuggling interdiction or reprocessing plant inspection. This is because

individual element decontamination factors will aid in nuclear forensics while examining the trace fission product contaminants in the smuggled plutonium.

ACKNOWLEDGEMENTS

I would like to thank Dr. Sunil Chirayath and Dr. David Boyle from the Nuclear Security Science and Policy Institute at Texas A&M for their support and expertise on this work. I would also like to thank Dr. Charles M. Folden III from the Cyclotron Institute at Texas A&M for his guidance and knowledge provided for the chemistry required throughout the course of this research.

Thanks also go to Mr. Paul Mendoza, Mr. Jeremy Osborn, and Dr. Jonathan Burns for providing assistance and advice over the course of this research. This work was performed under a joint NSF and DHS ARI program (NSF Grant No. ECCS-1140018 and DNDO-2012-DN-077-ARI1057-02&03) to carry out this research.

NOMENCLATURE

DUO_2	Depleted Uranium Dioxide
Pu	Plutonium
U	Uranium
PUREX	Plutonium Uranium Recovery by Extraction
BU	Burnup
TBP	Tri-n-Butyl Phosphate
HPGe	High Purity Germanium
MW	Megawatt
HM	Heavy Metal
FP	Fission Product
DF	Decontamination Factor
TRU	Transuranic
FBR	Fast Breeder Reactor
MWd	Megawatt Days
MWd/tHM	Megawatt Days per Ton of Heavy Metal
HFIR	High Flux Isotope Reactor
ORNL	Oak Ridge National Laboratory

TABLE OF CONTENTS

Page

LIST OF FIGURES

Page

LIST OF TABLES

Page

I. INTRODUCTION AND LITERATURE REVIEW

I.A. Introduction

India is in its final stages of completing its 500 MWe Prototype Fast Breeder Reactor (PFBR), scheduled to go critical by the end of 2016 [DAE, 2016]. Fast breeder reactors (FBRs) achieve a net increase in Pu, due to a conversion ratio greater than 1.0. Until now India has refused to accept international safeguards on this facility [Glaser, A., 2007]. Such actions have raised concerns, as these reactors have a "fertile blanket" consisting of depleted uranium (99.75% ^{238}U) around the core where plutonium can be produced. The total neutron fluence that the fertile blanket is exposed to is relatively low, leading to the production of weapons-grade plutonium (WGPu) [Doyle, J., 2008]. The PFBR blanket can then be reprocessed, and the plutonium recovered could potentially be misused for the purpose of weapons production. The potential to misuse the material generated in this type of reactor prompts interest in a detailed analysis of the fission products (FP) present in the separated plutonium and raffinate "waste" streams. A detailed understanding of these unique compositions would aid nuclear forensics activities for source attribution in the case of smuggled plutonium interdiction or at an inspection of a reprocessing plant to catch the misuse of such a plant.

The plutonium isotope of interest in WGPu is ^{239}Pu. The ^{239}Pu production by neutron capture in ^{238}U is through the following reaction;

$$^{238}_{92}U + ^{1}_{0}n \xrightarrow{(n,\gamma)} ^{239}_{92}U \xrightarrow[t_{\frac{1}{2}} = 23.5\ min]{\beta^-} ^{239}_{93}Np \xrightarrow[t_{\frac{1}{2}} = 2.4\ d]{\beta^-} ^{239}_{94}Pu$$

In this reaction after neutron capture, ^{239}U would beta decay to ^{239}Np and ^{239}Np would beta decay to ^{239}Pu [Baum et al., 2010]. The irradiated depleted uranium oxide (DUO_2) could also contain plutonium isotopes with mass numbers ranging from 238 to 242 depending on the duration of neutron irradiation in the reactor. The percentage of ^{239}Pu in plutonium (all isotopes) should be more than 93% to declare it as WGPu. In addition to the production of plutonium, minor actinides and uranium (remaining), FPs will be also present in the neutron-irradiated sample. Plutonium is generally separated from actinides and FPs using Plutonium-Uranium Recovery Extraction (PUREX) process. A typical PUREX flow sheet is shown in Figure 1 [Benedict et al., 1981]. The process consists of oxidation-reduction chemical reactions which utilize the oxidation states of plutonium dissolved in nitric acid and the solvent tri-n-butyl phosphate (TBP) to generate distinct streams of Pu and U separated from FPs contained in a neutron-irradiated uranium.

One of the goals of this work is to determine the FPs concentrations in the raffinate (waste) streams compared to the feed, as well as the trace FP contaminants that will accompany the plutonium product. The knowledge about these “contaminants” could identify a distinction between fast and thermal reactor plutonium product [Osborn, J., 2014]. These distinctions result from the differing neutron spectra present in these two reactors.

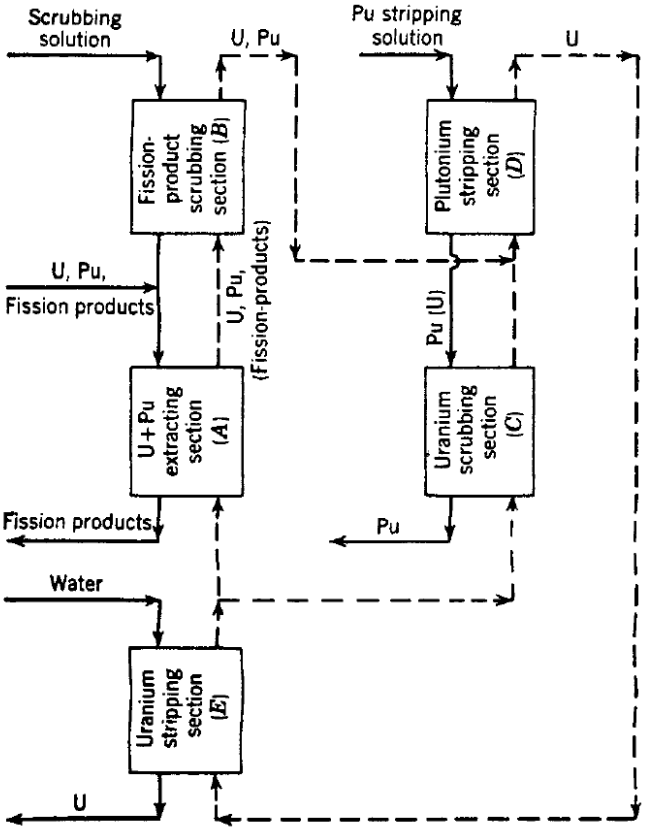

Figure 1. Example of a PUREX flowsheet (Solid lines are aqueous; Dashed lines are organic) [Reprinted with permission from Benedict et al., 1981].

In this work a bench-scale modified PUREX process was developed and used to greatly reduce the amount of FPs in the plutonium product. This modified PUREX process did not focus on purifying uranium product but instead focused on plutonium separation and its purification from FPs. Such a process will replicate, to the extent possible, the processes of larger reprocessing plants. By analyzing the concentrations of FPs in product and waste streams of the PUREX process, decontamination factors (ratio of contaminant/Pu in feed to contaminant/Pu in product) can be determined. This information will be useful in nuclear forensic analysis in the event of smuggled

plutonium interdiction as well as for determining the misuse of reprocessing plants from a nuclear safeguards perspective. For this project nuclear forensics is defined as the analysis of nuclear materials recovered from either the capture of unused materials, or from the radioactive debris following a nuclear explosion. Nuclear forensics can contribute significantly to the identification of the sources of the materials and the industrial processes used to obtain them [AAAS, 2008].

I.B. Literature Review and Previous Work

There have been many extensive publications on identifying nuclides for nuclear forensics analysis [Scott, M.R., 2005] [Glaser, A., 2009] [Wallenius et al., 2000] [Charlton et al., 2000]. A 2005 master's project completed at Texas A&M University identified nuclides that could be used to determine fuel age, burn-up, and enrichment of spent fuel that could be used for a radiological dispersal device (RDD) [Scott. M.R., 2005]. This work described potential reactor attribution applications, however it did not include any chemical processing of spent fuel.

There are considerable studies on the overall decontamination factors in the industrial scale PUREX process reprocessing facilities [Stoller et al., 1961] [Irish, E.R., 1959] [Irish et al., 1957] [Orth et al., 1963]. Decontamination factor refers to the cycle's ability to remove fission products and minor actinide elements from the plutonium product stream. These studies do not include results on the intermediate steps of the PUREX process or any analysis of smaller scale facilities. Such results are important for

understanding the intermediate PUREX process steps as well as process variation and how they affect the decontamination factors.

Additional nuclear forensics work has developed plutonium or fission product isotope analysis techniques to convey to investigators where a sample did not originate from. However, most of this research has focused on reactor spent fuel which has been irradiated to a high burn-up in which plutonium isotopic concentrations are no longer weapons grade. Investigations of isotopic concentrations of fission product contamination for low burn-up fuel from reactor misuse are also lacking [AAAS, 2008].

A forensics analysis for identifying various nuclear reactor types based on fission product contaminants in fuel discharged at a low burn-up was developed in a paper by S. Chirayath in 2015 [Chirayath et al., 2015]. This work involved reactor modeling and fuel burn-up simulations completed in 2014 and 2015 through thesis and dissertation efforts by J. Osborn and M. Swinney [Osborn, J., 2014] [Swinney, M., 2015]. The current thesis work was built off of these papers in order to develop experimental fission product contaminant forensics data for separated near weapons grade Pu that can be used in the future to identify PFBR blanket material that has been reprocessed using a PUREX process.

Information obtained through nuclear forensics analysis can be separated into two groups: endogenic information and exogenic information [Redermeier, A., 2009]. Endogenic information comes from within the sample; this includes sample age, nuclide concentrations, and morphology. Exogenic information comes from outside the sample; such information originates from comparisons with reference data/libraries. One of the

goals of this work is to present endogenic information, specifically unique fission product contaminants in separated plutonium using gamma spectroscopy analysis of PUREX-processed plutonium product and raffinate streams. This information could be used as exogenic information in future work to identify or exclude possible origins of nuclear material and could, most importantly, enhance U.S. investigative efforts as stated by the National Academy of Sciences in July 2010 [National Research Council, 2010].

II. METHODOLOGY

High resolution gamma spectroscopy was used to analyze the waste and product streams of the modified PUREX process. This non-destructive method of analysis provides relatively prompt results, and has become one of the key elements of international nuclear material safeguards.

The PUREX process was selected as the method of Pu separation due to its widespread use in reprocessing spent fuel in commercial facilities. This selection made sourcing the chemicals required for such a process easier. The concern however was this widespread use would also make it easier for potential proliferators at a larger scale facility to source the required chemicals. Along these lines, finding scientists with PUREX separation experience who would design/operate the facility would be more likely.

II.A. Non-Destructive Assay - High Resolution Gamma Spectroscopy

Gamma spectrometry is a fast characterization technique that can be used for nuclear forensics examination of seized nuclear or other radioactive material. This characterization technique owes its quick evaluation capability to the ease of making measurements and the fact that it is a non-destructive technique and requires minimal sample preparation. Detectors like high purity germanium (HPGe) can measure characteristic gamma rays (which are usually tightly spaced in energy with only a few keV or less between them) from the sample with a high energy resolution of ~2 keV with an accuracy up to $1/10^{th}$ of 1 percent. This highly resolved gamma energy spectrum will

provide the information required to quantify FP contaminant concentrations in Pu, which in turn can provide source reactor information and possibly sample age.

High energy resolution of the HPGe gamma spectroscopy system is governed by the variation in the number of charge carriers (electron-hole pairs) produced by the gamma rays in the detector through the photoelectric effect, variation in the charge carrier collection, and the contribution of electronic noise [Reilly et al., 1991]. For this thesis work, the HPGe detector energy and efficiency calibrations were performed using a 497.0 (±3.0%) nCi aqueous ^{152}Eu source in 1 mL of 0.5 M HCl from Eckert & Ziegler Isotope Products (assayed 15-Feb-12 12:00 PST). ^{152}Eu is a very useful radioisotope for determining the photo-peak efficiencies of an HPGe detector in the energy range of 122 keV to 1409 keV due to the multiple gamma-ray emissions from it (see Table 1). The traditional practice of using several standard sources for the above purpose is time consuming and multiple sources also introduce multiple sources of error when determining the efficiency of the system [Mukherjee et al., 1969], which can be avoided by using a ^{152}Eu source. The energy calibration was completed by fitting the measured centroids to the photopeaks of the known ^{152}Eu gamma energies as illustrated in Figure 2.

Table 1. ^{152}Eu gamma-ray energies used for detector calibration [KAERI, 2000].

Energy (keV)	Yield (%)	Uncertainty (%)
121.78	28.58	0.09
224.7	7.58	0.03
344.28	26.52	0.51
411.12	2.23	0.02
443.97	3.15	0.03
778.89	12.94	0.14
867.37	4.25	0.02
964.08	14.60	0.04
1112.07	13.64	0.04
1408.01	21.00	0.05

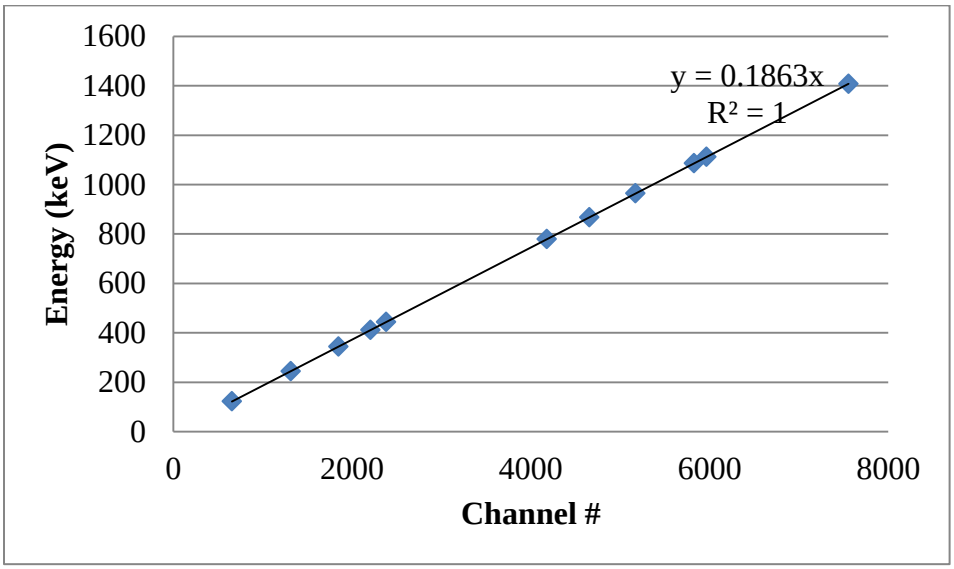

Figure 2. Energy calibration curve for Canberra Model GC4018 High-Purity Germanium (HPGe) detector surrounded by a lead cave designed to minimize background and the ^{152}Eu calibration source placed in a plastic vial holder 32 cm away from the detector head.

The efficiency calibration was performed using the calibration source's assayed activity, time since assay, gamma-ray energy yields, energy dependent photo-peak areas, and live count time. This calculation used Eq. 1, where C_n represent the number of counts under the photopeak curve for gamma-ray energy n, cutting off the Compton continuum and using the non-linear least squares method to fit the peak. T_L is the live count time of the sample. A_s is the activity of the calibration source after decay correction. γ_n is the yield or gamma-ray emission probability, n [Knoll, G.F., 2011].

$$\varepsilon = \frac{Counts}{T_L \, A_s \, \gamma_n} \tag{1}$$

In order to ensure an accurate calibration it is important to maintain the system geometry fixed. In this case the calibration source used was a 1 mL aqueous ^{152}Eu source. To maintain a similar geometry, the same vial type and liquid amount was used though each count. The efficiency calibration utilizes interpolation between energies used in the calibration curve seen in Figure 3. The method for interpolation is given in Eq. 2. This function relates the logarithm of the efficiency, ε to the logarithm of gamma-ray energy, E where a_i is a fitting parameter.

$$\ln(\varepsilon) = \sum_{i=1}^{N} a_i (\ln(E))^{i-1} \tag{2}$$

In this work calibrations used a 4th order polynomial ($N = 4$). The 4th order polynomial provided the best fit in this configuration according to errors produced by the

Canberra Industries' Genie 2000 gamma analysis software [GENIE, 2006] for the poly-fit function. The poly-fit function provided the a_i parameters that produced an agreeable curve fit through the least squares method.

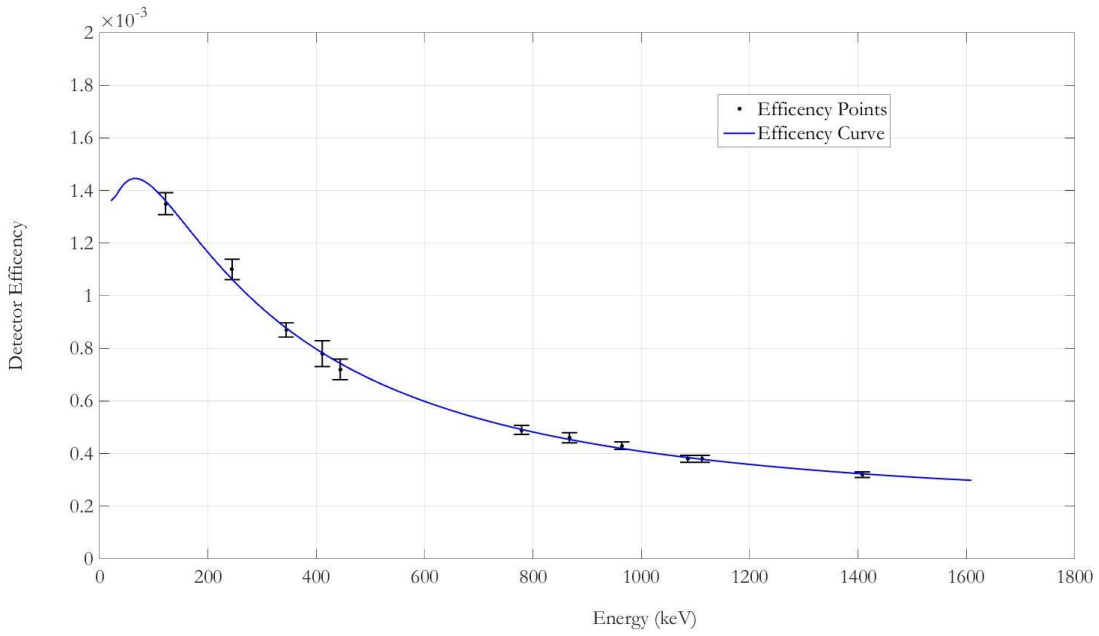

Figure 3. The efficiency calibration curve for the Canberra Model GC4018 High-Purity Germanium (HPGe) detector. A 1 mL aqueous ^{152}Eu calibration source 32 cm away from the detector head was used.

The activity of a particular nuclide was determined from the observed detector count rate by using Eq. 3.

$$A_n = \frac{C_n}{T_L \, \varepsilon_\gamma \, \gamma_n} \tag{3}$$

where A_n is the activity of nuclide n; C_n is the counts in the full-energy peak of the gamma-ray for nuclide n; T_L is the live count time of the measurement; ε_γ is the system

efficiency at a specific gamma-ray energy; and γ_n is the gamma-ray emission probability, or yield, of the gamma-ray for nuclide n.

In order to preclude false negative and false positive results, the smallest amount of activity the detector system can measure needs to be quantified. This detection limit was calculated using the critical value of the net instrument signal [MARLAP Ch 20, 2004]. This net instrument critical value (S_c) is defined per the relation in Eq. 4, where $\Pr[c_n > S_c \mid X = 0]$ indicates the probability that the observed net signal (c_n, which was calculated in Eq. 3) exceeds its critical value S_c when the analyte concentration (X) is zero. The significance level (α) is the probability of rejecting a null hypothesis when it is true (i.e. concluding that a difference exists from background when there is no actual difference). The significance level was set to the standard 5% level.

$$\Pr[c_n > S_c \mid X = 0] = \alpha = 0.05 \tag{4}$$

Since the background standard deviation for ROI i (σ_0^i) was not measured >20 times, an approximation of σ_0^i was required, denoted as $\hat{\sigma}_0^i$ [MARLAP Ch20, 2004]. $\hat{\sigma}_0^i$ is determined by a statistical evaluation with v degrees of freedom, so that the multiplier $Z_{1-\alpha}$ (the $(1-\alpha)$-quantile of the standard normal distribution) is replaced by $t_{1-\alpha}(v)$ which is the $(1-\alpha)$-quantile of the t-distribution with v degrees of freedom. As a result, Eq. 5 is transformed into Eq. 6.

$$S_c^i = Z_{1-\alpha}\,\sigma_0^i \tag{5}$$

$$S_c^i = t_{1-\alpha}(v)\,\hat{\sigma}_0^i \tag{6}$$

The $t_{1-\alpha}(v)$ value is found using a degree of freedom value that is equal to $(n-1)$, which denotes a value of one less than the number of independent measurements used to determine $\hat{\sigma}_0^i$. In this work 4 background measurements were made and a $t_{1-\alpha}(v)$ of 2.132 was used [MARLAP G-3, 2004]. This denoted a ~96% confidence limit. Once S_c^i was determined a gross instrument critical value y_c^i could be established (see Eq. 7), where $\hat{B}^i$ is the average of the background measurements for ROI i. The gross instrument critical value will be used as the response threshold to determine if the analyte concentration in a sample exceeds the blank measurement.

$$y_c^i = S_c^i + \hat{B}^i \tag{7}$$

II.B. Modified PUREX Process

The Plutonium-Uranium Recovery by Extraction (PUREX) process is a liquid-liquid (or solvent) extraction process used to separate the actinides plutonium and uranium from fission product contaminants in used nuclear fuel. Liquid-liquid extraction partitions solutes between two immiscible liquids. These two phases are initially mixed intimately to improve the rate of transfer of solutes between them. In the case of PUREX the aqueous phase consists of nitric acid (containing dissolved uranium, plutonium, other minor actinides, and fission products) and the organic phase consists of the tri-n-butyl phosphate (TBP) solvent extractant in a diluent, kerosene. A 30% concentration of TBP is used to prevent the formation of a third phase which would cause difficulty in the

extraction process [Morss et al., 2010]. TBP complexes with uranyl nitrate and tetravalent plutonium nitrate to selectively extract them to the organic phase. TBP coordinates with the uranium and plutonium to form a neutral complex which is soluble in the organic phase as depicted below [Benedict et al., 1981][Morss et al., 2010][Stoller et al., 1961].

$$UO_2{}^{2+}(aq) + 2NO_3{}^{-}(aq) + 2TBP(org) \rightleftharpoons UO_2(NO_3)_2 * 2TBP(org)$$

$$Pu^{4+}(aq) + 4NO_3{}^{-}(aq) + 2TBP(org) \rightleftharpoons Pu(NO_3)_4 * 2TBP(org)$$

However before the TBP contact an oxidizer needs to be added to the aqueous solution to ensure Pu is in its most extractable oxidation state, Pu(IV) [Morss et al., 2010]. In this work sodium nitrite ($NaNO_2$) was used as the oxidizer. Nitrogen dioxide (NO_2) was shown to be an effective oxidant while PUREX was under development [Connick, R. E., 1954] [Yost et al., 1946] [Brunstad, A., 1957]. Shown below is the oxidation scheme of Pu(III) that occurs with the NO_2 molecule.

$$Pu^{3+}(aq) + NO_2(aq) \rightarrow Pu^{4+}(aq) + NO_2{}^{-}$$

$$H^+ + NO_2{}^{-} \rightarrow HNO_2$$

$$HNO_2 + H^+ + NO_3{}^{-} \rightarrow 2NO_2 + H_2O$$

TBP can then be contacted with the aqueous phase to extract uranium and plutonium to the organic phase. Once uranium and plutonium are extracted to the organic phase, the organic phase needs to be separated from the FP-laden aqueous phase.

On an industrial scale this is done traditionally with a pulsed column or mixer-settler. A vortex mixer was used as a surrogate for the industrial scale mixer-settler depicted in Figure 4.

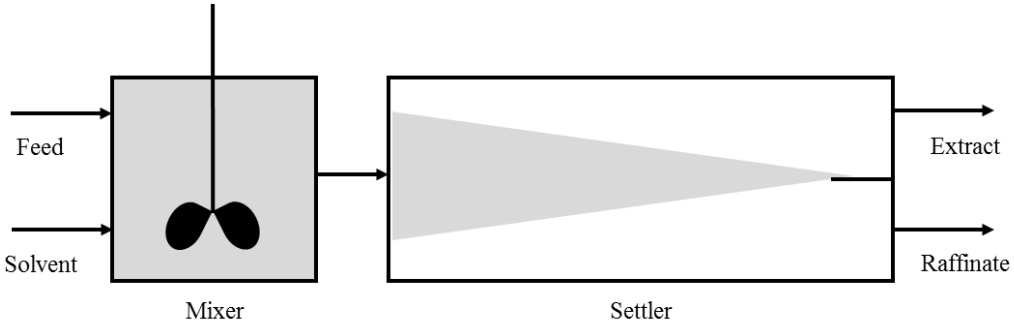

Figure 4. An industrial scale mixer-settler.

The vortex mixer will act as the mixing chamber. However unlike in a mixer-settler, the separation of phases occurs through centrifugal force. Similar to centrifugal contacts in a commercial reprocessing plant, the phases are separated using a bench-top centrifuge. This results in a more efficient and faster phase separation when compared to gravimetric settling where the phases separate by gravity.

The plutonium then needs to be partitioned from uranium. This is done through back-extraction of plutonium to an aqueous solution of nitric acid using Fe(II) sulfamate. The ferrous iron in the aqueous phase reduces plutonium from oxidation state IV to oxidation state III to be extracted into the aqueous phase as Pu(III) since it only weakly complexes with TBP [Irish et al., 1957].

$$Pu^{4+}(aq) + Fe^{2+}(aq) \rightleftharpoons Pu^{3+}(aq) + Fe^{3+}(aq)$$

One cycle of plutonium purification consisted of:

- Oxidation of Pu and U in 4 M HNO_3 by $NaNO_2$
- Contact of 30% TBP organic solution
- Removal of 30% TBP organic solution containing U and Pu (with minor fission product contamination)
- Back-extraction of Pu to aqueous phase by contact of $Fe_2(NH_2SO_3)_2$ in 0.75 M HNO_3 soln.
- Removal of 30% TBP organic solution containing U and FPs

This cycle will be repeated 3 times to ensure maximum FP and actinide decontamination. Decontamination of the plutonium product stream is quantified by a decontamination factor (DF) which is defined by taking a ratio of initial activity of a FP $(A_{in})_n$ in the feed to the final activity $(A_{out})_n$ of that FP in the desired purified product and normalized to a Pu recovery factor. This is described in Eq. 8 [Orth et al., 1963].

$$DF_n = \frac{(A_{in})_n}{(A_{out})_n} * \frac{(Pu)_{out}}{(Pu)_{in}} \tag{8}$$

It was assumed that there was 90% Pu recovery. This assumption was based on of results from similar extractions done in the lab that had been analyzed through mass spectroscopy [Mendoza et al., 2016]. Such an assumption was required as Pu could not be measured through gamma spectroscopy due to both the small amount of Pu and the very small gamma emission probability for ^{239}Pu (the most abundant Pu nuclide in this

case). Decontamination of plutonium from FPs does not occur to the same level for all FP nuclides due to the wide range of chemical properties among FPs.

II.B.1. Activity Balance and Distribution Ratios

The analysis of the reprocessing system can be done in a similar fashion as mass balance. In the case of the mass balance you are accounting for the material entering and leaving a system through mass measurements. By keeping track of the mass transfers in the system conservation of mass can be determined. Activity of radioactive material can be accounted for in a similar way, but instead of using mass measurements radioactivity is measured.

For this work the FP radioactivity content of the initial aliquot of stock solution (neutron irradiated DUO_2 dissolved in nitric acid) and the aqueous and organic phases were analyzed by gamma spectroscopy to ensure the radioactivity balance is maintained (see Eq. 9).

$$A_i = A_i^{org} + A_i^{aq} \tag{9}$$

where A_i is the initial solution activity for nuclide i, A_i^{org} is the organic phase solution activity for nuclide i, and A_i^{aq} is the aqueous phase solution activity for nuclide i. These A_i^{org} and A_i^{aq} values can both then be used to create a distribution ratio. The distribution ratio (D) or coefficient is the ratio of activity of an analyte in a solution with a mixture of two immiscible phases at equilibrium. This ratio is defined in Eq. 10 as the ratio of the analyte activity in each phase multiplied by the phase volume ratio at process step x

[Grahame et al., 1938]. This value will be used to quantify how well the analyte separates from a phase.

$$D_x = \frac{A_{i,x}^{org}}{A_{i,x}^{aq}} * \frac{V_x^{aq}}{V_x^{org}} \tag{10}$$

The distribution ratio provides a quantitative value for the efficiency of an extraction/back-extraction step for a particular analyte. The distribution ratio depends on several factors. These include the oxidation state of the analyte, the composition of the organic solution, the chemical form of the analyte being extracted, and the composition of the aqueous solution to name a few. In the context of nuclear forensics analysis it will be important to identify those nuclides which are difficult to remove from the product solution. These nuclides could potentially be used to develop a forensics profile for material that has used this method of reprocessing.

II.B.2. Fission Product and Actinide Decontamination

Another measure of efficiency for a reprocessing technique is the decontamination factor (DF), which can also be used to provide forensics information. The incomplete decontamination of fission products and other actinides from plutonium can provide characteristics of the chemical methods used in reprocessing as well as aid in plutonium-producing source reactor attribution. As mentioned in section II.B. and defined in Eq. 8, the decontamination of fission products and actinides is quantified using a decontamination factor. DF values of 10^6 to 10^7 have been reported previously

for gross gamma radioactivity after the traditional PUREX process [Irish et al., 1957]. Individual nuclide DF values have rarely been reported. More detailed elemental DF values are required for nuclear forensics analysis of interdicted plutonium samples and these are the objective of this work.

II.B.3. Reprocessing Technique Identification

Trace element compositions within reprocessed used nuclear fuel have been used before to attribute the material to a certain radiochemical process. For example the now obsolete REDOX process performed at Hanford would produce plutonium with a distinct contamination signature of ^{93}Zr. Whereas the BUTEX process performed at Windscale would produce plutonium with a distinct contamination of ^{106}Ru [Moody, K., 2008]. This work will look to confirm the distinct contamination signature of low-level rare earths in plutonium produced by a commercial-scale PUREX process.

II.C. DUO_2 Pellet Irradiation

This work focuses on the reprocessing characterization of a physical sample that represents the blanket material (DUO_2) irradiated in a FBR to a low-burn-up. In this case low-burn-up will be defined as less than 5 GWd/tHM. DUO_2 (0.2562 wt% ^{235}U) powder was supplied by AREVA and shaped into pellets by Oak Ridge National Laboratory (ORNL). The pellet dimensions were ~3 mm in diameter and ~0.2 mm thick. A FBR is not readily available in the US to irradiate a sample in a fast neutron spectrum. However an alternative approach was devised by placing the fuel samples inside a neutron

irradiation capsule ("Rabbit") that is surrounded with a gadolinium sheath which was then irradiated in the High Flux Isotope Reactor (HFIR) [Swinney, M., 2015]. HFIR is a flux-trap type reactor at ORNL. The gadolinium sheath would absorb the thermal neutrons resulting in a fast neutron to thermal neutron ratio of ~200 reaching the fuel samples inside the capsule. Figure 5 and Figure 6 illustrate the design of the rabbit and its elements.

The irradiation capsule was placed in position C-5 in the central flux target position in HFIR and vertical location 7 as depicted in Figure 7 & Figure 8. After irradiation the capsule was left to cool in the HFIR pool storage rack from June 1, 2013 prior to the shipment of the samples to Texas A&M University. The samples were received on August 31, 2013.

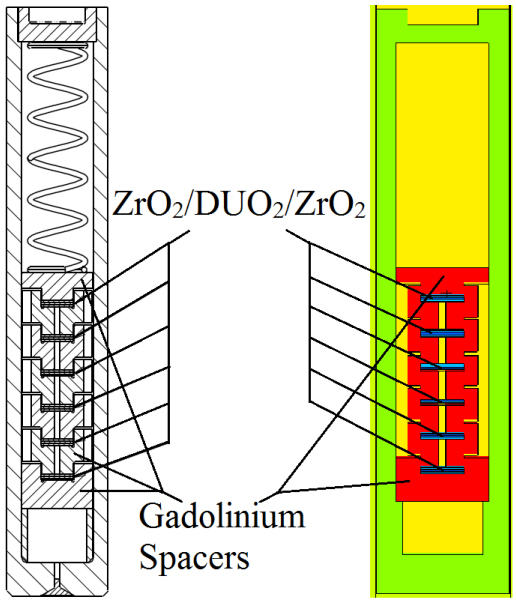

Figure 5. Irradiation capsule schematic and MCNP Model. ZrO_2 disks were used to reduce any interactions between the fuel samples and the gadolinium spacers.

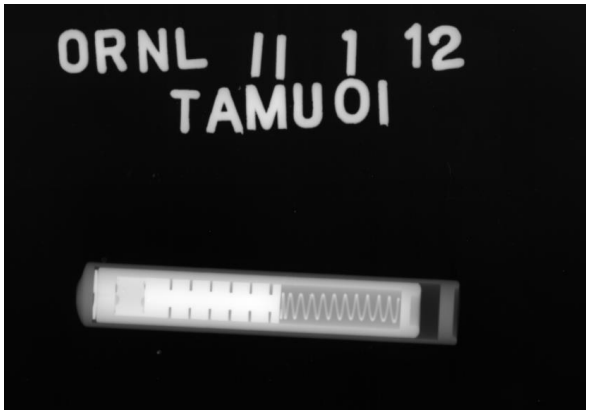

Figure 6. Radiograph of the capsule before irradiation at ORNL.

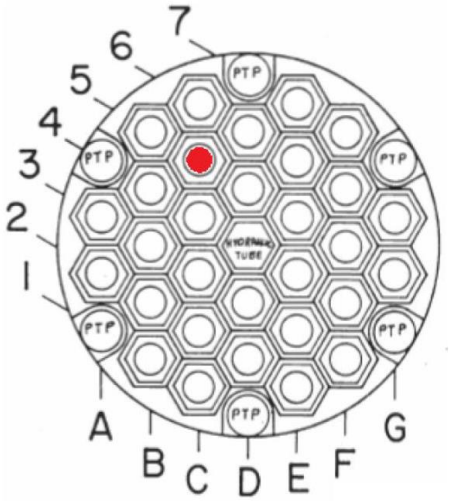

Figure 7. HFIR central flux target position identification schematic with the C-5 position highlighted.

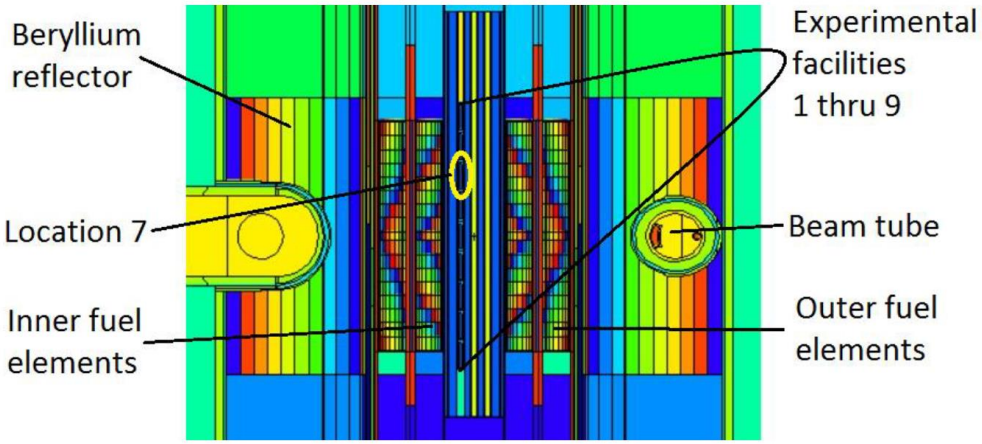

Figure 8. HFIR MCNP model illustrating the vertical experimental location in the flux trap region.

II.D. Pellet Dissolution

An eight-month decay period was allowed after the Nuclear Science Center (NSC) at Texas A&M University received the pellets on August 31, 2013. This allowed for the decay of many of the short-lived radioisotopes to reduce the radiation dose the dissolution personnel and experimentalist might receive. After the decay period the samples were transferred to a shielded glovebox at the NSC where the dissolution of one DUO_2 sample would occur. This sample was then weighed in a weighing boat on an electronic balance as depicted in Figure 9. The sample was found to weigh 12.9 ± 0.05 mg.

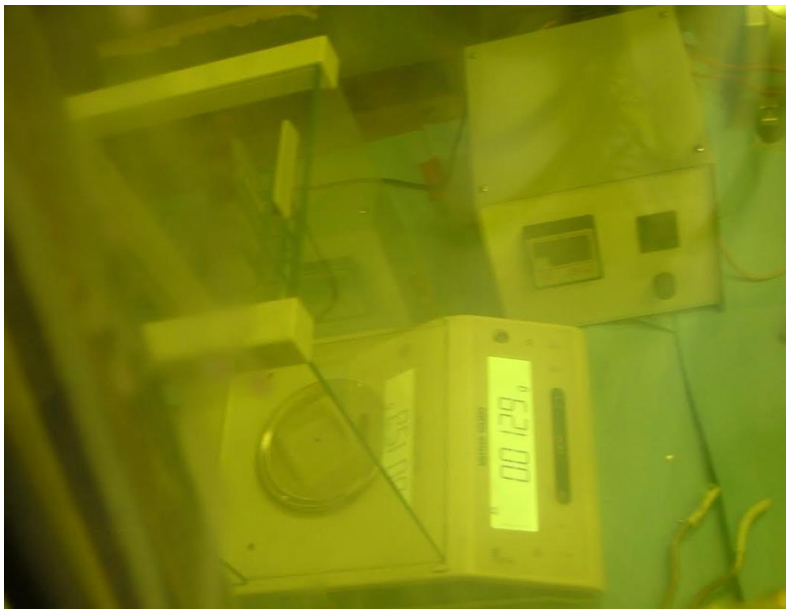

Figure 9. Weight measurement of the DUO_2 fuel sample inside the NSC glovebox.

The DUO_2 pellet was then transferred to a round bottom flask connected to a cold trap via a heated Schlenk line. The experimental setup is shown in Figure 10. 5 mL of 8 M HNO_3 was added to the round-bottom flask and the flask was heated to 50°C using a heating mantle from Electrothermal model EMA0100/CEBX1. This heating mantel contained a magnetic stirrer which also mixed the solution with constant 100 rpm for two hours.

A cold trap containing molecular sieves (Sigma-Aldrich (208574) 3 Å beads, 4-8 mesh) and surrounded by liquid nitrogen in a dewar was used to capture off-gases that were produced during the dissolution of the DUO_2 sample. This capture was facilitated by a Schlenk line which transferred the gases from the round bottom flask to the cold

trap. This Schlenk line was wrapped in heating tape to prevent condensation of these off-gases in the line.

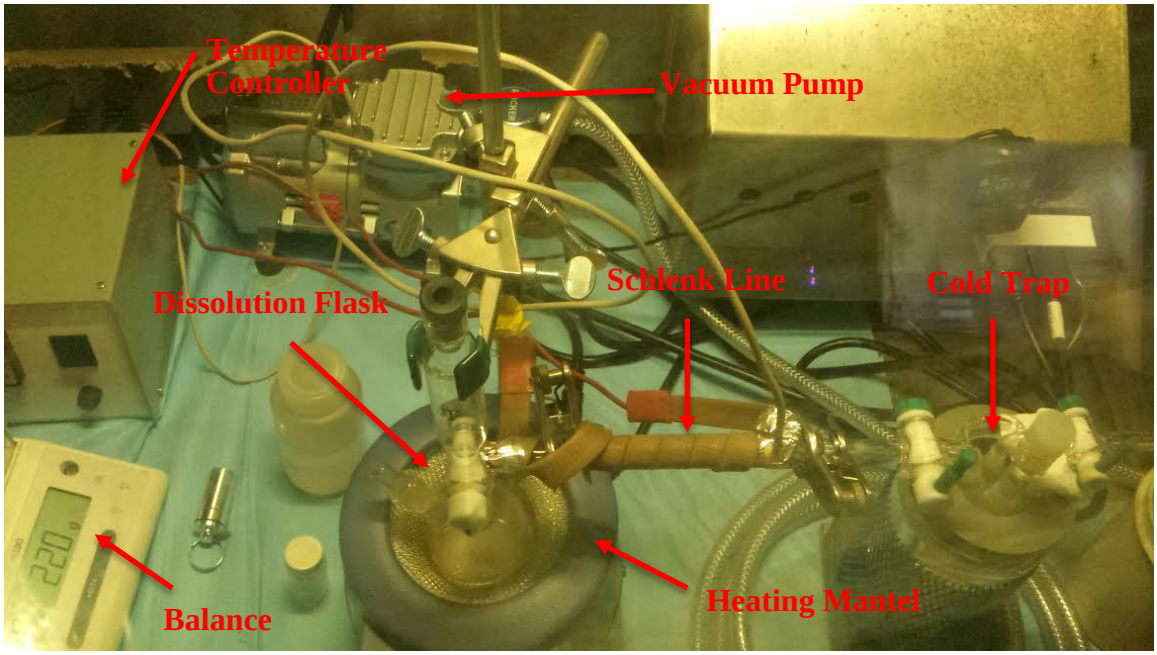

Figure 10. Experimental setup for dissolution of the DUO_2 pellet in the NSC glovebox.

Once the sample had been dissolved, the solution was transferred to a 20 mL glass scintillation vial and kept heavily shielded. This solution was referred to as the "dissolution solution." This lead pig was then transferred from the NSC to the Nuclear Forensics & Radiochemistry Laboratory on the main Texas A&M campus. In order to reduce the dose that one would receive while performing radiochemical separations a 500 µL aliquot from the dissolution solution was diluted to 5 mL and adjusted to 4 M HNO_3. This diluted solution was named the "stock solution" and was stored in its own 20 mL glass scintillation vial in a lead pig.

III. EXPERIMENTAL PROCEDURE AND RESULTS

III.A. Modified PUREX Process

As previously mentioned the initial dissolved solution and stock solutions were stored in 20 mL glass scintillation vials with urea caps from Fisher Scientific. The radiochemical separations of the modified PUREX process were performed in 15 mL VWR ultra high performance centrifuge conical-bottom tubes made of ultra-clear polypropylene copolymer with caps made of high density polyethylene. VWR 50 mL centrifuge tubes were used for storing the prepared solutions which included 4 M nitric acid, the 30% TBP solution, and iron(II) sulfamate solution. When these vials were not in use, the caps were wrapped in parafilm to seal and reduce evaporation losses.

A mBraun LABmaster Pro Glove Box Workstation with two glove stations and an approximate volume of 1.4 m^3 was used in the Nuclear Forensics & Radiochemistry Laboratory to provide an inert gas working environment for these experiments. Radiacwash Towelettes from BioDex Medical Systems Inc. were used periodically on the gloves and centrifuge tubes to clean up any accidental contamination. The inert gas atmosphere of the glovebox was maintained by argon gas from Praxair, and the molecular sieve filtration medium was regenerated using a hydrogen/argon mix from the same supplier.

Inside the glovebox, shielding was provided by an L-Block leaded glass shield from Biodex, standard 2”x4”x8” lead bricks, and a lead pig used to store the stock solution.

Operations within the glovebox were performed with a Fisher Scientific Digital Vortex Mixer, an Ample Scientific Centrifuge model Champion F-33D, an Eppendorf 1000 µl adjustable pipette with dual filter 1250 µl certified clean and sterile purity grade tips, and a standard 4”x6” ring stand.

Chemicals used included distilled water for dilution from an Elga Purelab flex water purification system model PF3XXXXM1; Kerosene ($C_{12}H_{24}$) used as the TBP diluent obtained from Alfa Aesar (L14479-500mL), Lot # J28X018; Sodium nitrite ($NaNO_2$) obtained from Sigma-Aldrich (563218-25G), Lot # MKBP2493V (≥99.999 % purity); TBP ($(CH_3(CH_2)_3O)_3PO$) obtained from Fluka Analytical (00675-100mL), Lot#: BCBD7470V (≥99.0 % purity); Nitric Acid (HNO_3) obtained from EMD Millipore (NX0408-7-250mL), Lot # 52027 (69% concentration); and Fe(II) Sulfamate ($Fe(NH_2SO_3)_2$) obtained from Strem Chemicals (93-2638), Lot # 18170000 (40.26% concentration).

Three prepared solutions were created in a fume hood before separation chemistry occurred. This included a 25 mL solution of 0.024 M iron(II) sulfamate with 0.75 M nitric acid; a 30 mL solution of 4 M nitric acid; and a 30 mL solution of 30 % TBP in kerosene. These solutions were reused throughout the modified PUREX process displayed in Figure 11.

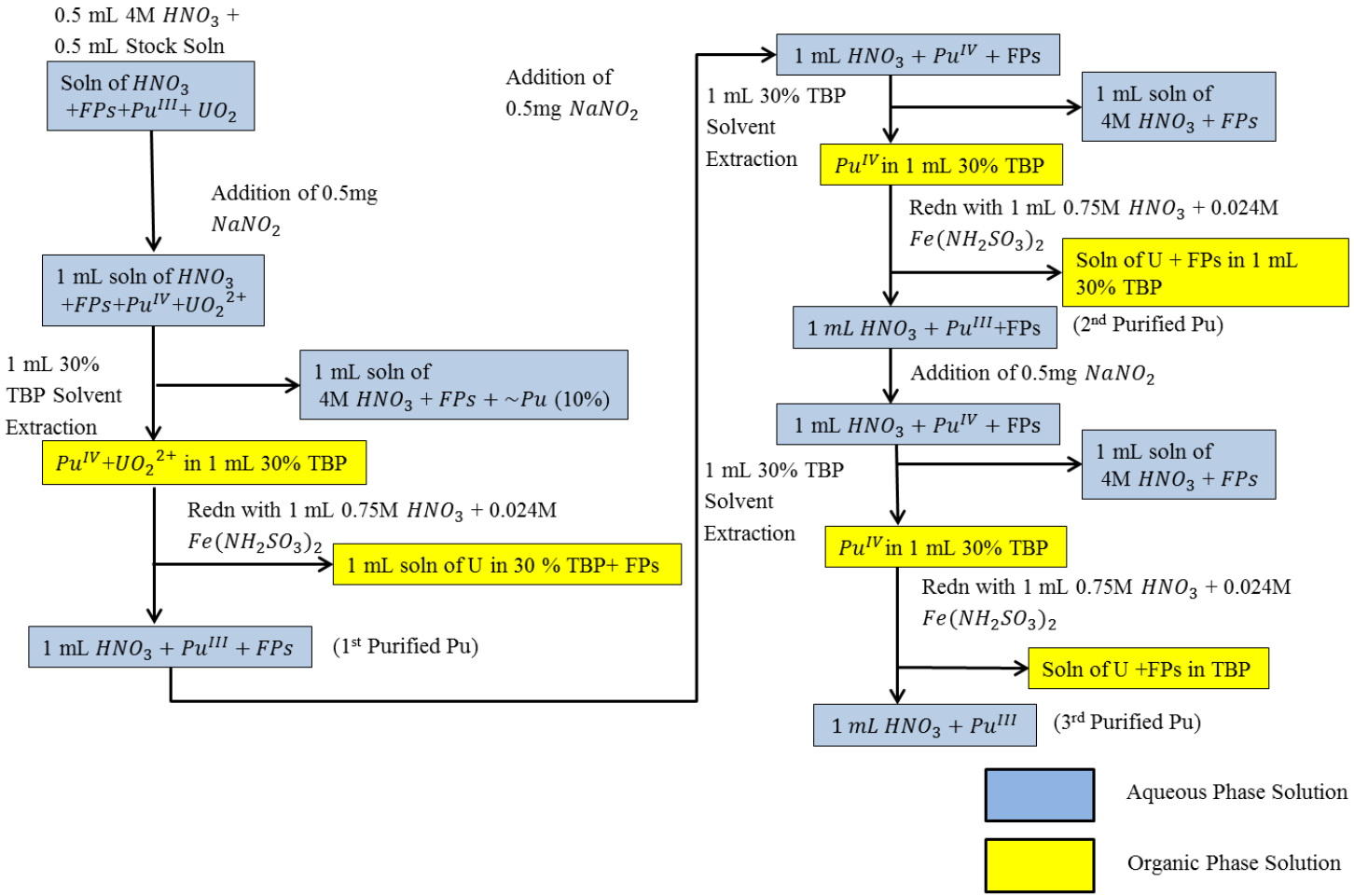

Figure 11. Modified PUREX process with three stage plutonium purification.

The modified PUREX process began, as stated earlier, by using a 500 μL aliquot of the stock solution (containing ~1% of the original irradiated DUO_2 contents). To ensure equal volumes later in the procedure 500 μL of 4 M nitric acid was added to the 500 μL stock solution. This 1 mL aliquot's Pu(III) was converted to Pu(IV) by adding ~0.5 mg of sodium nitrite via plastic scoopula with subsequent stirring, and covering. The solution was left overnight (~16 h) to be completely oxidized to Pu(IV).

The 1 mL aliquot was then contacted with 1 mL of 30% by volume TBP, diluted in kerosene, at room temperature. Afterwards, the 2 mL solution was mixed using a vortex mixer at 1500 rpm for 15 minutes to thoroughly mix the two phases. Afterwards, the solution was centrifuged at 3000 rpm for 15 minutes separating the two phases. The TBP organic phase was then removed to the maximum extent possible and placed in a separate vial. This organic phase removal was done through two 250±10 μL and then three 125±5 μL transfers using the adjustable pipette, resulting in a small reduction in volume. This was done to ensure part of the aqueous phase was not extracted with the organic phase.

The back-extraction of Pu from the organic phase occured in a similar manner by contacting the 1 mL solution with a 1 mL dilute nitric acid solution containing Fe(II) sulfamate. Again this 2 mL solution was mixed using a vortex mixer at 1500 rpm for 15 minutes to thoroughly mix the two phases. Afterwards, the solution was centrifuged at 3000 rpm for 15 minutes separating the two phases. The TBP organic phase was removed as before and placed in a separate vial which should contain the majority of uranium.

This plutonium purification cycle (extraction and back-extraction) was repeated two more times in order to purify plutonium. During each of these steps the vials containing ~1 mL of solution (organic and aqueous streams) were analyzed via an HPGe gamma detector. In this fashion the separation of Pu from fission products could be monitored and quantified. A step by step procedure of this process is described in Appendix B.

III.B. Gamma Spectroscopy Measurements

Throughout the modified PUREX process gamma spectroscopy measurements were taken at each stage (such as initial feed, separated organic and aqueous phases for each purification cycle, etc.) of each vial containing the solution from the process steps. Measurements were taken using a Canberra Model GC4018 High-Purity Germanium (HPGe) detector surrounded by a lead cave designed to minimize background as seen in Figure 12. Sample vials were placed in a custom built plastic vial holder that was placed at 32 cm from the detector head (see Figure 13). Before the start of the experiment, calibration and background measurements were taken using the detector setting listed in Table 2. As mentioned earlier an aqueous ^{152}Eu source with an activity of 433 nCi (497±0.5 nCi on 2/15/2012) was used for energy and efficiency calibrations of the system. This source was placed in the same position and vial as the samples to be measured for a more accurate calibration.

Table 2. Information and settings on the HPGe detector.

HPGe Model:	Canberra GC4018
Serial #:	10210
Bias:	+3500 V
Energy Range:	0 to 1.5 MeV
Rise Time:	8.8 μs
Flat Top:	1.2 μs

Figure 12. HPGe detector with elongated lead cave used to reduce background interference.

Figure 13. Plastic vial holder and 15 mL vial for reference inside lead cave.

Several nuclides of interest were measured using gamma spectroscopy through the stages of the modified PUREX process. The activities of these nuclides are calculated using Eq. 3. The live count time (T_L) was determined by subtracting the real counting time (T_R) by the dead time (T_D) as described in Eq. 11. The error for this value was quantified using Eq. 12 and a 1E-5% error in both T_D and T_R.

$$T_L = T_R - T_D \tag{11}$$

$$\sigma_{T_L} = \sqrt{\left(\sigma_{T_R}\right)^2 + \left(\sigma_{T_D}\right)^2} \tag{12}$$

The maximum dead time observed was 1.32%, giving rise to a 98.68% live time. Such dead time was acceptable and was the reason for the 32 cm distance that the

sample was placed at from the detector head. When the sample was placed at 8 cm from the detector head a dead time of 15.6% was observed, necessitating the longer distance.

As discussed in section II.A., the detection limits of this detector system were calculated using the critical value of the net instrument signal (S_c). The net gamma events recorded by the detector system, also called net counts, for ROI i (c_n^i) is defined as the total (gross) counts at ROI i (c_T^i) minus the gross critical value for detection for ROI i (y_c^i) (see Eq. 13). The values for the gross critical value are shown in Table 3. For nuclides that had multiple ROIs a weighted average was taken to produce a single critical value per nuclide of interest.

Table 3. The gross critical values (S_c) and levels (y_c) for the nuclides of interest.

Nuclide	**Critical Value (S_c) (cps)**	**Critical Level (y_c^i)(cps)**	**Error (±)**
Cs-137	7.28	98.3	5.8
Ce-144	60.92	102	15
Sb-125	6.69	8.5	1.8
Eu-154	9.39	12.9	2.9
Zr-95	8.29	13.7	3
Rh-106	87.33	918.0*	54

* 511 keV positron annihilation energy elevates background

The error of this value is quantified using Eq. 14. Error is a result of the Gaussian fit to the peak and random background events.

$$c_n^i = c_T^i - y_c^i \tag{13}$$

$$\sigma_{c_n^i} = \sqrt{\left(\sigma_{c_T^i}\right)^2 + \left(\sigma_{y_c^i}\right)^2} \tag{14}$$

The total relative error for the activity of ROI i is defined in Eq. 15. Gamma-ray emission probability error comes from the evaluated nuclear data sourced from the National Nuclear Data Center (NNDC) at Brookhaven National Laboratory. The error of the detector efficiency is determined through the Genie peak-fit method [GENIE, 2006].

$$\sigma_{A_i} = |A_i| \sqrt{\left(\frac{\sigma_{c_n^i}}{c_n^i}\right)^2 + \left(\frac{\sigma_T}{T}\right)^2 + \left(\frac{\sigma_{\varepsilon_\gamma}}{\varepsilon_\gamma}\right)^2 + \left(\frac{\sigma_{\gamma_i}}{\gamma_i}\right)^2} \tag{15}$$

The nuclides presented in Table 4 were chosen because they had gamma-ray emission energies within the efficiency calibration (between 122 keV and 1408 keV). These gamma-ray emissions were free of significant interferences (this is a potential problem in irradiated fuel measurements) from peak overlap, and had relatively large gamma yields with well documented nuclear data. The large chemical variation of these nuclides (^{137}Cs is an alkali metal; ^{154}Eu and ^{144}Ce are lanthanides; ^{95}Zr is a transition metal; ^{125}Sb is an amphoteric element; and ^{106}Ru is a platinum metal) was beneficial in quantifying the differences in their decontamination factors and distribution ratios in the PUREX process.

Table 4. Nuclides of interest.

Nuclide	Gamma-ray Energy (keV)	Emission Probability	Error (±)	Half-Life
^{154}Eu	1274.43	0.3483	0.003	8.593 y
^{144}Ce	133.5	0.1109	0.0019	284.91 d
^{125}Sb	427.9	0.296	-	3.892 y
^{137}Cs	661.7	0.851	0.002	30.08 y
^{95}Zr	756.73	0.5438	0.0022	64.02 d
^{106}Ru* (^{106}Rh)	511.86	0.204	-	371.8 d

*^{106}Ru beta decays to ^{106}Rh which has an instantaneous 511.86 keV gamma emission

Figure 14 illustrates a gamma spectrum from a 1.0 mL initial solution containing 0.5 mL stock solution (~1% of dissolved irradiated DUO_2 pellet) and 0.5 mL of 4 M HNO_3 in a 15 mL vial that was placed in a plastic holder within the lead cave 32 cm from the detector face. For nuclides with multiple gamma-ray peaks, the activity for each peak was calculated, then an average was calculated for that isotope's activity.

For each plutonium purification cycle of the modified PUREX process multiple gamma-ray measurements were performed. An additional measurement of the 0.5 mL stock solution with added 0.5 mL 4 M nitric acid was performed before the first purification cycle. The multiple measurements for each cycle included:

- Measurement of aqueous phase after TBP contact
- Measurement of organic phase after TBP contact
- Measurement of aqueous phase after Fe(II) sulfamate back-extraction
- Measurement of organic phase after Fe(II) sulfamate back-extraction

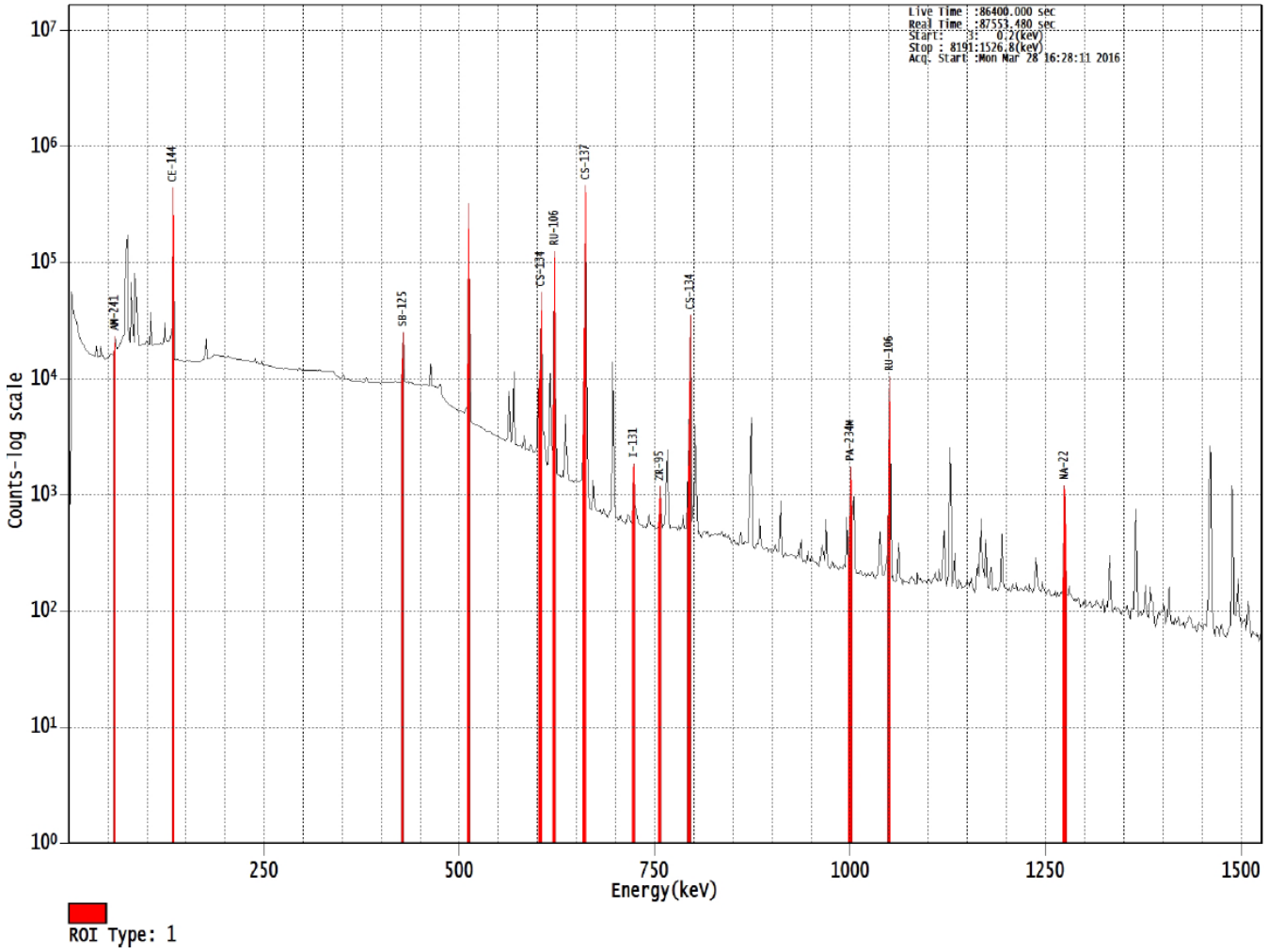

Figure 14. An example of the gamma spectrum from the dissolved DUO_2 stock solution.

III.B.1. Activity Balance

Throughout the modified PUREX process, it was important to track the flow of activity. The measurable activity of the fission products provided a process check and these values were used to calculate the distribution coefficient and decontamination factors. The notable pathways of activity included the transfer to the organic phase after a TBP contact, the transfer of activity from the organic phase to the aqueous phase after back-extraction using Fe(II) sulfamate, and residual activity left on the pipette tips after organic phase removal.

For activities that were unbalanced due to a phase having an activity below the critical value (quoted in Table 3) for detection (described as not detectable (ND)) a summation methodology was implemented as shown in Eq. 16, where A_i is a measurable initial activity; $A_i^{measurable}$ is a phase containing a measurable activity; and A_i^{ND} is the phase that was ND. The error of A_i^{ND} is the relative error of the ND phase activity (which was calculated before the critical level was subtracted from it) with the addition of the critical level error.

$$A_i - A_i^{measurable} = A_i^{ND} \tag{16}$$

Table 5 displays the measured activity for ^{137}Cs. The additional activity data for the other nuclides of interest appear in Appendix A. The initial activity for the 1st TBP contact process step was the measured activity of the stock solution aliquot. For each process step after, the initial activity of the process step was the measured activity from the Pu product stream.

Table 5. Measured data for activities of ^{137}Cs.

Nuclide	Step	Initial Activity (Bq)	Error(±)	Aqueous Activity (Bq)	Error(±)	Organic Activity (Bq)	Error(±)
Cs-137	1st TBP Contact	87100	7000	83000	6700	602	49
	1st Fe(II) Contact	602	49	551	45	26.3	2.2
	2nd TBP Contact	551	45	539	44	11.4	1.1
	2nd Fe(II) Contact	11.4	1.1	ND	-	ND	-
	3rd TBP Contact	-	-	-	-	-	-
	3rd Fe(II) Contact	-	-	-	-	-	-

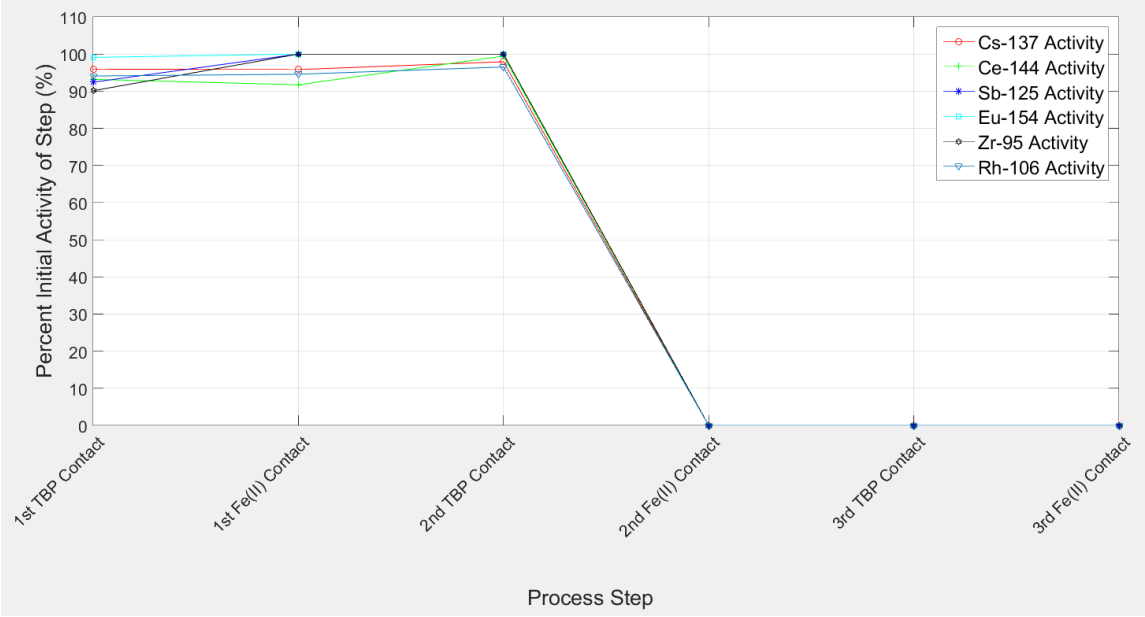

Figure 15. Remaining initial activity normalized to the initial process step activity for 6 nuclides that were tracked through the modified PUREX process. (See the main text for discussion)

The total activity for a process step i is denoted as A_i^T, which is the summation of the organic and aqueous phase activities for process step i described in Eq. 17. The absolute error for the summation of activity within a process step is denoted as $\sigma_{A_i^T}$ and defined in Eq. 18. A_i^T was normalized to the initial activity of the process step and reported as a percent and is shown in Figure 15. The figure is meant to depict the activity accountancy for each process step and helped to check for activity losses through the modified PUREX process.

$$A_i^T = A_i^{org} + A_i^{aq} \tag{17}$$

$$\sigma_{A_i^T} = \sqrt{\left(\sigma_{A_i^{org}}\right)^2 + \left(\sigma_{A_i^{aq}}\right)^2} \tag{18}$$

After the second TBP contact the activity of the nuclides of interest drop below the minimum detection activity of the detector. This is the reason for the plots in Figure 15 dropping to 0% after this step. Variations between 90% and 100% of the initial activity were results of losses that occurred during the experiment through residue left on the pipette tips as well as the peak-fit validation method used in gamma spectroscopy measurements. With ^{154}Eu and ^{95}Zr it is assumed that the remaining activity in the 1st Fe(II) contact remained in the organic phase. This was required to maintain the activity balance after the concentrations had dropped below the lower limit of detection.

III.B.2. Distribution Ratios

As stated in Eq. 10 the distribution ratio (D_i^x) takes a ratio of activity in the organic phase and divides it by the activity in the aqueous phase. This ratio also incorporates a volume correction factor, which takes into account the unequal volumes of the phases measured. The relative error of the distribution ratio for process step x and the nuclide corresponding to gamma energy i is defined in Eq. 19.

$$\sigma_{D_i^x} = |D_i^x| \sqrt{\left(\frac{\sigma_{A_{org}^x}}{A_{org}^x}\right)^2 + \left(\frac{\sigma_{A_{aqu}^x}}{A_{aqu}^x}\right)^2 + \left(\frac{\sigma_{V_{org}^x}}{V_{org}^x}\right)^2 + \left(\frac{\sigma_{V_{aqu}^x}}{V_{aqu}^x}\right)^2} \qquad (19)$$

Low D values for FPs were desired in the 1st TBP contact of the modified PUREX process. This would indicate that the majority of the contaminate fission products would be left in the raffinate stream. Of the fission products analyzed, cesium was expected to most readily remain in the raffinate stream [Schulz, W.W., 1984]; this was confirmed in experimental data shown in Table 6, with ^{137}Cs and ^{125}Sb producing the lowest and 2nd lowest D values, respectively. Poor decontamination was seen for ^{95}Zr and ^{106}Ru, which displayed the highest and 2nd highest D values in this process step. Such results were generally in agreement with previous reports [Schulz, W.W., 1984] [Benedict et al., 1981] [Irish et al., 1957].

Table 6. Distribution ratios after the 1st TBP contact of the 4 M nitric acid stock solution in the modified PUREX process.

1st TBP Contact	Cs-137	Ce-144	Sb-125	Eu-154	Zr-95	Rh-106
Distribution Ratio (D)	0.0073	0.0177	0.0092	0.0277	0.078	0.0379
Error(±)	0.0008	0.0013	0.0022	0.0077	0.017	0.0033

In the stripping/back-extraction step, dilute nitric acid with Fe(II) sulfamate was expected to produce higher distribution ratios when compared to the TBP contact step. This result would indicate that FPs would remain in the organic phase while the product Pu will be transferred back to the aqueous phase. The Fe(II) reduces Pu(IV) in TBP to Pu(III) which causes it to fall out from the organic TBP phase to the aqueous phase. Also the dilute concentration of nitric acid used in Fe(II) sulfamate aids in the separation of the nitrate bonded cations of interest. However, the Fe(II) reduction and dilute nitric acid concentration can also causes other impurities to fall out of the organic phase as well, the most notable being ^{137}Cs and ^{144}Ce as seen in Table 7. The best separation occurred for ^{125}Sb and ^{95}Zr which remained in the organic phase most readily.

Table 7. Distribution ratios after the 1st Fe(II) contact of the modified PUREX process using a 0.75 M HNO_3 solution.

1st Fe(II) Contact	Cs-137	Ce-144	Sb-125	Eu-154	Zr-95	Ru-106
Distribution Ratio (D)	0.0478	0.0419	0.77	0.37	0.48	0.337
Error(±)	0.0056	0.0056	0.42	0.55	0.12	0.030

III.C. Decontamination/Fission Product Purification Factor

TBP coordinates to metals via its phosphoryl group, with the oxygen atom forming coordinate links with cations as displayed in Figure 16. These adducts or solvates are neutral extractants; the best characterized of these is $UO_2(NO_3)_2 \bullet 2TBP$ [Schulz, W.W., 1984]. There are many other extractant species that are less studied. Therefore it is critical to reduce the amount of variability in the system to better define the behavior of these extractants within the modified PUREX process.

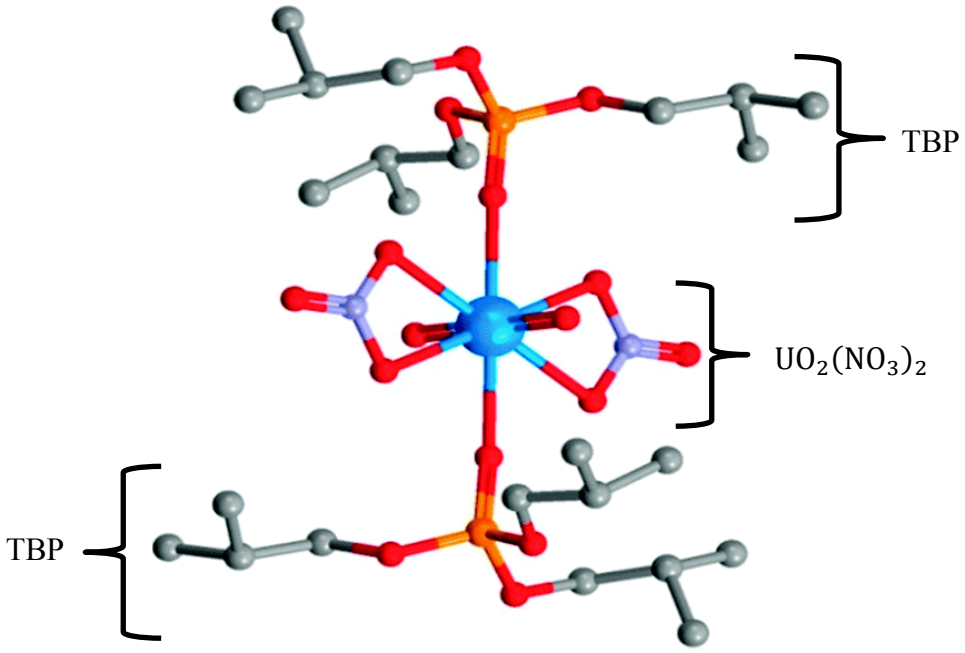

Figure 16. Structure of $UO_2(NO_3)_2 \bullet$TBP from single crystal X-ray diffraction [Wilson et al., 2013].

Maintaining equal volumes is one of these variability reduction techniques implemented. It was crucial for the activity balance to maintain equal volumes of the two

phases due to the variation that occurs in detected activity because of the source geometry change. It was also found that a centrifuge is necessary to expedite and more completely separate the two phases (organic and aqueous). Initially, using the gravimetric settling, two phases reformed in the partitioned organic phase resulting in a poor decontamination factor. It was found that the change in geometry from a 0.5 mL aqueous sample to a 1 mL sample and lack of complete phase separation resulted in a 93.6±7.7% difference when comparing the initial activity of a process step to the summation of the two phase activities after phase separation, illustrating the importance of these variability reduction techniques.

After the three plutonium purification cycles of the modified PUREX process, the resulting decontamination from fission products and minor actinides are reported in Table 8 by purification cycle. (Cycle 3 is not presented as all of its values were under the critical level of detection). The elements were grouped based on their location on the periodic table to better understand their chemical behavior through the chemical separations. In the 2nd cycle it was noted that the activity measured from the back-extraction step was less than the critical value (S_c) for detection. This required the use of the critical value as the $(A_{out})_n$ value, resulting in the small DF values of the 2nd cycle. This would denote a lower limit of decontamination. Theoretically, if the critical level of detection were lower the DF values for this cycle would be the same as the first cycle DF values. The total DF values were determined by using the initial activity of each nuclide and dividing that by the critical level (shown in Table 3) that corresponded to that nuclide.

Table 8. Decontamination factors (DFs) of the nuclides of interest after each modified PUREX cycle (assumed 90% Pu recovery).

Nuclide	1st Cycle	Error(±)	2nd Cycle*	Error(±)	Total	Error(±)
Cs-137	142	12	5.04	0.37	798	58
Sb-125	189	58	2.8	1.4	600	250
Ce-144	63.0	4.7	22.0	6.9	1540	480
Eu-154	46	13	1.42	0.67	73	28
Zr-95	20	16	1.43	0.55	32	10
Ru-106	37.0	3.6	4.51	0.38	186	16

* $(A_{out})_n$ was lower than the critical detection limit, requiring the critical level (y_c^i) to be used in its place resulting in a lower limit of decontamination.

Through the 1st cycle, ^{95}Zr is one of the more troublesome fission products to decontaminate from the plutonium product. In an aqueous solution of HNO_3, zirconium (a 4d-transition metal) exists mainly in the 4+ oxidation state and forms of ZrO^{2+} which can complex into $Zr(NO_3)_4 \bullet 2TBP$, as described in Eq. 20, and travel with Pu to the organic phase [Gupta, C.K., 2003].

$$ZrO^{2+}(aq) + 2H^+(aq) + 4NO_3^- + 2TBP(org) \rightleftharpoons Zr(NO_3)_4 \bullet 2TBP(org) + H_2O \quad (20)$$

Due to this TBP complexation, ^{95}Zr has a poor DF after the first purification cycle. The distribution of zirconium into organic solvents under process conditions is the largest of the observed fission products and actinides in Table 6. This D value is large enough to cause difficulty in obtaining a satisfactory decontamination which is observed in Table 8.

Ruthenium can exist in all oxidation states from 2+ to 8+ within the process steps [Stoller et al., 1961]. The main Ru nuclide of concern is ^{106}Ru. ^{106}Ru is a fission product

and is grouped as a platinum metal; it is known to exhibit complex chemistry in HNO_3 due to the formation of multiple nitrato- and nitro- complexes that can inter-convert [Pruett, D.J., 1984]. This causes ^{106}Ru and its daughter product ^{106}Rh to be the second most troublesome nuclide to remove from the product stream behind ^{95}Zr. This can be seen in the DF and D-values presented in Table 8 and Table 6 where both indicate that ^{106}Ru is the second most difficult nuclide to remove in this modified PUREX process in the 1^{st} cycle.

Antimony (^{125}Sb) is an amphoteric fission product and exists in process solutions mainly in the 3+ oxidation state [Stoller et al., 1961]. As shown in Table 8, it is not appreciably extracted into the organic solvent, and this produces the highest DF value for the 1^{st} Pu purification cycle. The relatively high error of the ^{125}Sb DF value is a result of the error associated with the low aqueous phase activity.

Cerium and europium, both lanthanide fission products, exist in nitric acid in the 3+ oxidation state [Stoller et al., 1961]. Because of this oxidation state, ^{144}Ce and ^{154}Eu displayed a low to moderate extractability into the organic TBP phase when compared to the other nuclides of interest. ^{144}Ce posed a greater problem in the back-extraction step, where it had a much lower D-value than ^{154}Eu resulting in more ^{144}Ce moving to the aqueous phase with plutonium.

Cesium, an alkali metal fission product, is not appreciably extracted into organic solvents [Stoller et al., 1961]. The nuclide of interest in this case is ^{137}Cs. ^{137}Cs, is produced proportionally to the integrated neutron flux [Reilly et al., 1991]. It was

observed that ^{137}Cs achieved the 2nd highest total DF value. The majority of this decontamination came from the good separation ^{137}Cs had in the TBP extraction step.

IV. CONCLUSIONS

In this experiment the goal was to mimic an industrial PUREX process for microgram plutonium quantities and decontaminate the product stream plutonium from a dissolved solution of fast-spectrum-irradiated depleted uranium dioxide. A bench-scale modified PUREX process was developed which implemented a three-cycle purification process to partition fission products from the product plutonium. This goal was achieved after the 3rd purification cycle for all of the nuclides of interest based on the critical detection limit of the detection system.

It was observed through measured distribution ratios that ^{95}Zr and ^{106}Ru were the most difficult nuclides (of the analyzed nuclides) to prevent from entering the product stream during the TBP contact step. In the aqueous raffinate stream, ^{137}Cs and ^{125}Sb remained most readily. In contrast, during the Fe(II) sulfamate contact, ^{137}Cs and ^{144}Ce were the most difficult to remove from the product stream. It was also observed that ^{95}Zr and ^{125}Sb remained in the organic raffinate stream most readily during this back-extraction process. Based on these data, future unknown samples containing ^{137}Cs and ^{144}Ce in the aqueous product stream from the back-extraction and ^{95}Zr and ^{106}Ru in the TBP product stream could help identify the separation process as PUREX.

Based on the calculated decontamination factors, ^{137}Cs and ^{144}Ce were the most readily removed nuclides from the product stream when analyzing the complete 1st purification cycle (TBP contact and Fe(II) back extraction). This performance was indicated by higher DF values. ^{95}Zr and ^{106}Ru were shown to be the most difficult to remove through the 1st cycle of purification based on their low DF values.

The use of an activity balance indicated that no more than 10% of any nuclide's detected activity was removed from the system through pipette tip holdup or other loss factors, the error of which was based on detector efficiency, gamma-ray emission probability, peak fitting, and count time.

IV.A. Future Work

In future work mass spectroscopy will be used to quantify the amount of plutonium in the end product plutonium vials to determine the efficiency of this three-cycle PUREX purification process. The very low gamma-ray emission probability for Pu gamma rays made it very difficult to quantify the Pu amounts through gamma spectroscopy. The next step in this forensics effort is the irradiation of natural uranium dioxide pellets, which will be used to simulate spent fuel discharged from a pressurized heavy water reactor (PHWR). Once irradiated, these pellets will undergo a similar PUREX process as the PFBR pellet performed in this work. The results of this reprocessing will be compiled into a database to confirm specific nuclide characteristics that could be used to identify the reactor used to produce the irradiated fuel, which supplied weapons-grade plutonium.

REFERENCES

Baum, E. M., Knox, H. D., & Miller, T. R. (2010). *Nuclides and Isotopes: Chart of the Nuclides.* Niskayuna, NY: Knolls Atomic Power Laboratory (KAPL).

Benedict, M., Pigford, T., Levi, H. (1981). *Nuclear Chemical Engineering* (2nd ed.). New York, NY: McGraw-Hill.

Brunstad, A. (1957). *Oxidation of Plutonium (III) by Sodium Nitrite* (HW-51655). Richland, WA: General Electric Co. Hanford Atomic Products Operation.

Charlton, W. S., Fearey, B. L., Nakhleh, C. W., Parish, T. A., Perry, R. T., Poths, J. et al. (2000). Operator Declaration Verification Technique for Spent Fuel at Reprocessing Facilities. *Nuclear Instruments and Methods in Physics Research, 168*(B), 98-108.

Chirayath, S. S., Osborn, J. M., & Coles, T. M. (2015). Trace Fission Product Ratios for Nuclear Forensics Attribution of Weapons-Grade Plutonium from Fast and Thermal Reactors. *Science & Global Security*, *23*(1), 48-67.

Connick, R. E. (1954). *Oxidation States, Potentials, Equilibria, And Oxidation-Reduction Reactions of Plutonium* (National Nuclear Energy Series IV-l4A). New York, NY: McGraw-Hill.

Department of Atomic Energy (DAE). 2016, Fast Breeder Reactors. http://pib.nic.in/newsite/PrintRelease.aspx?relid=142349

Doyle, J. (2008). *Nuclear Safeguards, Security and Nonproliferation: Achieving Security with Technology and Policy.* Amsterdam ; Boston : Butterworth-Heinemann.

Genie 2000 Spectroscopy Software: Operations Manual (2006). (V3.1. ed.). Meriden, CT: Canberra Industries, Inc.

Glaser, A. (2009). Isotopic Signatures of Weapon-Grade Plutonium from Dedicated Natural Uranium-Fueled Production Reactors and Their Relevance for Nuclear Forensics Analysis. *Nuclear Science and Engineering, 163* (1), 26-33.

Glaser, A., & Ramana, M. V. (2007). Weapon-Grade Plutonium Production Potential in the Indian Prototype Fast Breeder Reactor. *Science and Global Security, 15*(2), 85-105.

Grahame, D. C., & Seaborg, G. T. (1938). The Distribution of Minute Amounts of Material Between Liquid Phases. *Journal of the American Chemical Society, 60(10)*, 2524-2525.

Gupta, C. K. (2003). Chemical Metallurgy: Principles and Practice. (pp. 521). Mumbai, India: Wiley-VCH Verlag GmbH & Co. KGaA, Weinheim.

Irish, E. R. (1959). *Description of PUREX Plant Process* (HW-60116). Richland, WA: Hanford Atomic Products Operation.

Irish, E., & Reas, W. (1957). *The PUREX Process- A Solvent Extraction Reprocessing Method for Irradiated Uranium* (HW-49483A). Richland, WA: General Electric Co. Hanford Atomic Products Operation.

Knoll, G.F. (2011) *Radiation Detection and Measurement*. (4^{th} ed.) Hoboken, NJ: Wiley.

Koning, A., Forrest, R., Kellett, M., Mills, R., Henriksson, H., & Rugama, Y. (2006). *The JEFF-3.1 Nuclear Data Library*. JEFF Report 21. Boulogne-Billancourt, France: OECD.

Korea Atomic Energy Research Institute (KAERI) Nuclear Data Center Table of Nuclides. (2000). http://atom.kaeri.re.kr:8080/ton/index.html

MARLAP Manual: Appendix G, Statistical Tables. (2004). (pp. G-3). NUREG-1576. Washington, DC: U.S. Nuclear Regulatory Commission.

Mendoza, P. M., Chirayath, S. S., & Folden III, C. M. (2016). Fission Product Decontamination Factors for Plutonium Separated by PUREX from a Low-Burnup, Fast-Neutron Irradiated Depleted UO_2. *Submitted to Applied Radiation and Isotopes.*

Moody, K. (2008). Forensic Radiochemistry. *UCRL-PRES-214033*. Berkeley, CA: University of California Radiation Laboratory.

Moody, K., Hutcheon, I., & Grant, P. (2005). *Nuclear Forensic Analysis.* Boca Raton, FL: Taylor & Francis Group, LLC.

Morss, L., Edelstein, N., & Fuger, J. (2010). *The Chemistry of the Actinide and Transactinide Elements.* (4th ed.). New York, NY: Springer.

Mukherjee , P., & Sengupta, A. K. (1969). ^{152}Eu as a Calibrating Source for Ge(Li) Detectors. *Nuclear Instruments and Methods in Physics Research, 68(1)*, 165-166.

Multi-Agency Radiological Laboratory Analytical Protocols Manual: (MARLAP) (2004). Washington, DC: U.S. Nuclear Regulatory Commission.

National Research Council. Nuclear Forensics: A Capability at Risk (Abbreviated Version). Washington, DC: The National Academies Press, 2010.

NNDC Chart of the Nuclides. Brookhaven National Laboratory. http://www.nndc.bnl.gov/chart/

Nuclear Forensics In Support of Investigations: Implementing Guide (2015). IAEA Nuclear Security Series No. 2-G (Rev.1). Vienna: International Atomic Energy Agency (IAEA).

Nuclear Forensics: Role, State of the Art and Program Needs (2008). Washington DC: AAAS/APS.

Orth, D., & Olcott, T. (1963). PUREX Process Performance versus Solvent Exposure and Treatment. *Nuclear Science and Engineering, 17*(4), 593-612.

Osborn, J. (2014). Trace Fission Product Ratios for Nuclear Forensics Attribution of Weapons-Grade Plutonium from Fast Breeder Reactor Blankets. (Master of Science, Texas A&M University).

Pruett, D. J. (1984). *The Solvent Extraction of Heptavalent Technetium and Ruthenium by Tributyl Phosphate.* US DOE rept. ORNL/TM-8668. Oak Ridge National Laboratory.

Redermeier, A. (2009). *Fingerprinting Of Nuclear Material for Nuclear Forensics*. ESARDA Bulletin, No. 43. European Safeguards Research and Development Association.

Reilly, D., Ensslin, N., & Smith Jr, H. (1991). *Passive Nondestructive Assay of Nuclear Materials (PANDA)* Los Alamos National Laboratory.

Safety Reports Series: Safe Handling and Storage of Plutonium. (1998). No.9. Vienna: International Atomic Energy Agency.

Sampson, T. E., & et al. (1982). Plutonium Isotopic Composition by Gamma-Ray Spectroscopy. *Nuclear Instruments and Methods in Physics Research, 193*(1-2), 177-183.

Schulz, W. W. (1984). *Science and Technology of Tributyl Phosphate Vol. 1 Synthesis, Properties, Reactions and Analysis*. Boca Raton, FL: CRC Press.

Scott, M. R. (2005). Nuclear Forensics: Attributing The Source of Spent Fuel Used in an RDD Event. (Master's Thesis, Texas A&M University).

Solovkin, A. S. (1974). Thermodynamics of Extraction of Tetravalent Plutonium, Uranium, Thorium and Zirconium. *Journal of Radioanalytical Chemistry, 21*(1), 15-29.

Stoller, S., & Richards, R. (1961). *Reactor Handbook, Volume II, Fuel Reprocessing*. New York, NY: Inter Science Publishers, Inc.

Swinney, M. (2015). Experimental and Computational Assessment of Trace Nuclide Ratios in Weapons Grade Plutonium for Nuclear Forensics Analysis. (Doctor of Philosophy, Texas A&M University).

Wallenius, M., Peerani, P., & Koch, L. (2000). Origin Determination of Plutonium Material in Nuclear Forensics. *Journal of Radioanalytical and Nuclear Chemistry,* 246(2), 317-321.

Wilson, A. M., Bailey, P. J., Tasker, P. A., & et al. (2014). Solvent Extraction: The Coordination Chemistry behind Extractive Metallurgy. *Chem. Soc. Rev., 43*(1), 123-134. Published by The Royal Society of Chemistry.

Yost, D. M., & Russell Jr., H. (1946). *Systematic Inorganic Chemistry*. New York, NY: Prentice-Hall, Inc.

APPENDIX A

NUCLIDE ACTIVITIES

Table 9. Measured data for activities of ^{144}Ce.

Nuclide	Step	Initial Activity (Bq)	Error(±)	Aqueous Activity (Bq)	Error(±)	Organic Activity (Bq)	Error(±)
Ce-144	1st TBP Contact	175200	8800	160400	8000	2840	150
	1st Fe(II) Contact	2840	150	2500	130	105	13
	2nd TBP Contact	2500	130	2490	130	14.1	5.8
	2nd Fe(II) Contact	14.1	5.8	ND	-	ND	-
	3rd TBP Contact	-	-	-	-	-	-
	3rd Fe(II) Contact	-	-	-	-	-	-

Table 10. Measured data for activities of ^{125}Sb.

Nuclide	Step	Initial Activity (Bq)	Error(±)	Aqueous Activity (Bq)	Error(±)	Organic Activity (Bq)	Error(±)
Sb-125	1st TBP Contact	5640	390	5160	360	48	11
	1st Fe(II) Contact	48	11	26.9	7.1	21	10
	2nd TBP Contact	26.9	7.1	23.4	8.1	3.4	4.4
	2nd Fe(II) Contact	3.4	4.4	ND	-	ND	-
	3rd TBP Contact	-	-	-	-	-	-
	3rd Fe(II) Contact	-	-	-	-	-	-

Table 11. Measured data for activities of ^{154}Eu.

Nuclide	Step	Initial Activity (Bq)	Error(±)	Aqueous Activity (Bq)	Error(±)	Organic Activity (Bq)	Error(±)
Eu-154	1st TBP Contact	1042	53	1005	53	27.9	7.6
	1st Fe(II) Contact	27.9	7.6	20.3	5.1	7.6	11
	2nd TBP Contact	20.3	5.1	12.2	2.5	8	3.5
	2nd Fe(II) Contact	8	3.5	ND	-	ND	-
	3rd TBP Contact	-	-	-	-	-	-
	3rd Fe(II) Contact	-	-	-	-	-	-

Table 12. Measured data for activities of ^{95}Zr.

Nuclide	Step	Initial Activity (Bq)	Error(±)	Aqueous Activity (Bq)	Error(±)	Organic Activity (Bq)	Error(±)
Zr-95	1st TBP Contact	490	28	409	26	32.1	6.7
	1st Fe(II) Contact	32.1	6.7	21.7	4.4	10.4	1.6
	2nd TBP Contact	21.7	4.4	18.5	4.8	3.19	0.84
	2nd Fe(II) Contact	3.19	0.84	ND	-	ND	-
	3rd TBP Contact	-	-	-	-	-	-
	3rd Fe(II) Contact	-	-	-	-	-	-

Table 13. Measured data for activities of ^{106}Ru (^{106}Rh).

Nuclide	Step	Initial Activity (Bq)	Error(±)	Aqueous Activity (Bq)	Error(±)	Organic Activity (Bq)	Error(±)
Ru-106	1st TBP Contact	190000	12000	172000	11000	6510	400
	1st Fe(II) Contact	6500	400	4600	280	1553	97
	2nd TBP Contact	4600	280	3800	240	646	41
	2nd Fe(II) Contact	646	41	ND	-	ND	-
	3rd TBP Contact	-	-	-	-	-	-
	3rd Fe(II) Contact	-	-	-	-	-	-

APPENDIX B

CHEMISTRY PRODECURES

Experiment J Procedure (Modified PUREX Process)

**The information in parentheses refers to sample identification numbers.*

1. Leach plastic vials to be used with 3% HNO_3 overnight
2. Create a 0.024 M $Fe(NH_2SO_3)_2$ +0.75 M HNO_3 solution (2 J)
    a. 25 mL : 1.2145 mL 15.44 M HNO_3 + 0.2605 mL 2.302 M $Fe(NH_2SO_3)_2$ + 23.525 mL DI H_2O
3. Use a 30 % TBP solution (3 I)
    a. 30 mL : 21 mL kerosene + 9 mL TBP
4. Use a 4 M HNO_3 solution (4 J)
    a. 30 mL : 7.772 mL 15.44 M HNO_3 + 22.228 mL DI H_2O
5. Create a 1.0 mL dissolved pellet solution using a 0.5 mL aliquot of 4 M HNO_3 from (4 J) + 0.5 mL aliquot of dissolved pellet stock solution from glass scintillation vial (5 J)
6. Perform a background count with empty 15 mL vial
7. Count vial (5 J) containing the 1.0 mL aliquot of stock solution
8. Add 0.5 mg of $NaNO_2$ to vial (5 J) stock solution
9. Shake (5 J) in vortex mixer at 1500 rpm for 15 min
10. Let sit overnight for complete oxidation (~8 hrs)
11. Contact (5 J) with a 1.0 mL aliquot of 30 % TBP solution (3 I)
12. Shake (5 J) in vortex mixer at 1500 rpm for 15 min
13. Centrifuge for 15 min at 3000 rpm for phase to separation
14. Remove Organic TBP phase (top) from (5 J), transfer to (6 J)
15. Count (5 J) containing the aliquot of aqueous phase solution
16. Count (6 J) containing the aliquot of organic phase solution
17. Contact (6 J) with a 1.0 mL aliquot of 0.024 M $Fe(NH_2SO_3)_2$ +0.75 M HNO_3 solution (2 I)
18. Shake (6 J) 1500 rpm for 15 min
19. Centrifuge for 15 min at 3000 rpm for phase to separation
20. Remove Organic TBP phase (top) from (6 J) and transfer to (7 J)
21. Count (6 J) containing the aliquot of aqueous phase solution
22. Count (7 J) containing the aliquot of organic phase solution
23. Add 0.5 mg of $NaNO_2$ to vial (6 J) (oxidizes Pu(III) back to Pu(IV))

24. Shake (6 J) in vortex mixer at 1500 rpm for 15 min
25. Let sit overnight for complete oxidation (~8 hrs)
26. Contact (6 J) with a 1.0 mL aliquot of 30 % TBP solution (3 I)
27. Shake (6 J) in vortex mixer at 1500 rpm for 15 min
28. Centrifuge for 15 min at 3000 rpm for phase to separation
29. Remove Organic TBP phase (top) from (6 J) to (8 J)
30. Count (6 J) containing the aliquot of aqueous phase solution
31. Count (8 J) containing the aliquot of organic phase solution
32. Contact (8 J) with a 1.0 mL aliquot of 0.024 M $Fe(NH_2SO_3)_2$ +0.75 M HNO_3 solution (2 I)
33. Shake (8 J) in vortex mixer at 1500 rpm for 15 min
34. Centrifuge for 15 min at 3000 rpm for phase to separation
35. Remove Organic TBP phase (top) from (8 J) to (9 J)
36. Count (8 J) containing the aliquot of aqueous phase solution
37. Count (9 J) containing the aliquot of organic phase solution
38. Add 0.5 mg of $NaNO_2$ to vial (8 J)
39. Shake (8 J) in vortex mixer at 1500 rpm for 15 min
40. Let sit overnight for complete oxidation (~8 hrs)
41. Contact (8 J) with a 1.0 mL aliquot of 30 % TBP solution (3 I)
42. Shake (8 J) in vortex mixer at 1500 rpm for 15 min
43. Centrifuge for 15 min at 3000 rpm for phase to separation
44. Remove Organic TBP phase (top) from (8 J), transfer to (10 J)
45. Count (8 J) containing the aliquot of aqueous phase solution
46. Count (10 J) containing the aliquot of organic phase solution
47. Contact (10 J) with a 1.0 mL aliquot of 0.024 M $Fe(NH_2SO_3)_2$ +0.75 M HNO_3 solution (2 I)
48. Shake (10 J) 1500 rpm for 15 min
49. Centrifuge for 15 min at 3000 rpm for phase to separation
50. Remove Organic TBP phase (top) from (10 J) and transfer to (11 J)
51. Count (10 J) containing the aliquot of aqueous phase solution
52. Count (11 J) containing the aliquot of organic phase solution